ARCHIVES OF TRANSPORT *ISSN (print):* *0866-9546*
Volume 68, Issue 4, 2023 ***e-ISSN (online):*** *2300-8830*
DOI: *10.61089/aot2023.bw74g958*

CAPABILITIES TO USE PASSIVE MEASUREMENT SYSTEMS TO DETECT OBJECTS MOVING IN A WATER REGION

Waldemar MIRONIUK[1], Krystian BUSZMAN[2]

[1, 2] *Polish Naval Academy, Gdynia, Poland*

Abstract:

The increase in the use of sea water is the basis for the development of the existing security systems in given areas. Monitoring the navigational situation in a given water area is one of the most important tasks aimed at ensuring the necessary level of safety in maritime traffic. Marine surveillance systems at sea are used for this purpose. As an interesting approach related to the study of the movement of vessels, this paper proposes a method based on the measurement of physical field disturbances generated by objects moving in the sea water. These disturbances can be referred to the upper (air space) and lower (underwater) hemisphere. In the upper hemisphere the motion of the object generates disturbances of the thermal field while in the lower hemisphere disturbances of the acoustic, hydrodynamic, magnetic, electric and seismic fields are generated. Detection of the floating objects and determination of movement parameters is realized mainly by active systems. There are radiolocation systems in the upper hemisphere (radar systems) and echo ranging systems in the lower hemisphere (sonars and echosounders). Monitoring of the upper hemisphere of sea vessels traffic is conducted in a comprehensive manner. The lower hemisphere is in the most cases omitted. Therefore, it is recommended to develop underwater observation systems as a source of additional information about floating objects and thus complement the existing systems used in navigation. However, at present, despite the technological progress, there is a noticeable lack of the comprehensive solutions in the area of monitoring the vessels movement in the underwater space. Therefore, appropriate action should be taken to recognize this technology gap and increasing the safety of vessel traffic. The aim of the article was to present a fully passive, mobile underwater observation system that uses a number of sensors to monitor the underwater environment parameters, the research methodology and analysis of the obtained results. The method of deploying the measurement system at the selected geographical position and the measurement method are described. Based on obtained results, the analysis of sound pressure disturbances caused by passing ships was performed. A feature extraction method was developed to identify a passing vessel based on low frequency signal parameters.

Keywords: *sea transport safety, underwater observation system, ship detection, ship classification, hydroacoustic parametrization*

To cite this article:

Mironiuk, W., Buszman, K., (2023). Capabilities to use passive measurement systems to detect objects moving in a water region. Archives of Transport, 68(4), 137-156. https://doi.org/10.61089/aot2023.bw74g958

Contact:
1) w.mironiuk@amw.gdynia.pl [https://orcid.org/0000-0001-7931-3680] – corresponding author; 2) k.buszman@amw.gdynia.pl [https://orcid.org/0000-0002-3724-9091]

1. Introduction

The sea area plays an important role in human life. The human activities related to the sea include, first of all: transport (Önden et al., 2023; Wu et al., 2019), energy extraction (Esteban et al., 2020; Klabučar et al., 2020; O'Kelly-Lynch et al., 2020), natural resources extraction from the seabed (Blanchard et al., 2023; Van Elden et al., 2019; Zhang et al., 2019), fishing along with fish and shellfish farming (Delgado et al., 2018; Leonart 2008; Ruiz-Salmón et al., 2021; Widyaningrum, Masruroh 2012), naval activities or recreation (Danzell et al., 2023); Queiroz Pereira, Correia Dantas 2019. Most of the above-mentioned activities is concentrated in the coastal zone. There is an increased movement of various vessels in it. It applies to both small, recreational boats as well as to large-size commercial vessels (Gucma, Marcjan 2012; Pelot, Plummer 2008). The latter move along strictly designated approach lines to the civilian harbors. Moreover, increase of people migration and trade by sea have contributed to substantial increase in traffic on sea lanes. More than 80% of the world trade makes use of maritime transport, which has become one of the pillars of international trade. Apart from many advantages, it is created several hazards to safety in maritime transport and to natural environment even using the newest technology.

High density of vessels requires detailed and accurate monitoring of the traffic within that area of water region. Monitoring of the navigational situation in a particular water body is one of the most important tasks aimed at ensuring the necessary level of safety in the sea traffic (Jingxiang et al., 2023; Xuri et al., 2023; Mou et al. 2019). For this purpose, dedicated systems are used to observe moving floating objects (Fiuk at al., 2022). These systems are still dynamically developing, which allows for obtaining more complete and accurate spatial information. The development of navigation situation monitoring systems involves both specific operating parameters (e.g., the use of high-resolution images in radar systems (Weimin et al., 2023)), the use of synthetic aperture systems (Pleskachevsky et al., 2022; Ustalli et al. 2022), and the introduction of new solutions in the form of the use of different methods of filtering or coded signal transmission, or neural networks (Zhang et al., 2023).

An object moving in the water depth is a source disturbance of the local physical fields resulting from changes in its position. These disturbances can be referred to the upper (air space) and lower (underwater) hemisphere. In the upper hemisphere the motion of the object generates disturbances of the thermal field (J. J. Holmes 2022; Li et al. 2023) while in the lower hemisphere disturbances of the acoustic, hydrodynamic, magnetic, electric and seismic fields are generated (Wołoszyn et al. 2022; Tarnawski et al. 2021; Buszman 2020).

Detection of the floating objects and determination of movement parameters is realized mainly by active systems. These are radiolocation systems in the upper hemisphere (radar systems (Loran et al. 2023)) and echo ranging systems in the lower hemisphere (sonars and echosounders (Jeong et al., 2012)). Passive systems, which include underwater observation systems, are less used than airborne systems.

Navigation of the surface vessels is oriented primarily on acquiring of the necessary information from active detection systems of the upper hemisphere. In this space, electromagnetic (EM) waves serve as the transmission medium. Navigational data acquired from the receivers of radionavigation, radar and other radio-electronic devices, which are part of the vessels on-board navigation systems, are sent to the traffic management systems in maritime areas, so called VTS (Vessel Traffic Service) (De Bièvre 1985; Stach et al., 2023). VTS consists of a control centre, observation systems, and communications. They belong to the group of Vessel Monitoring Systems (VMS) (Watson 2016). By design, they integrate radioelectronic systems such as: AIS (Automatic Identification System), RADAR with ARPA system, VHF, NAVTEX and other subsystems. They are used to visualize the navigational situation. Monitoring of the selected area requires the integration of a large amount of data from distributed and different observation systems and sensors (Kazimierski at al., 2017; Smirnova 2018). The recorded information from distributed sources, their imaging and supervision translate directly into shortening the crew's reaction time in case of a threat e.g., collision (Blok 2018). In such a situation, the time of decision making by the watch officer regarding e.g., change of the movement direction or speed of the vessel is very important (Mironiuk 2015). Thus, the expected level of safety at sea must be constantly improved, e.g. by developing ship traffic monitoring systems.

As can be seen from the information described above, monitoring of the upper hemisphere in terms

of sea vessels traffic is conducted in a comprehensive manner.

The lower hemisphere is in the most cases omitted, what is caused by ranges of underwater systems, especially based on electromagnetic waves (Aman et al., 2022; Aman et al., 2023). Exceptions are systems that base their operation only on a hydroacoustic field, such as gliders (Tessei A. et al. 2015).

Therefore, it is recommended to develop underwater observation systems as a source of additional information about floating objects and thus complement the existing systems used in navigation. However, at present, despite the technological progress, there is a noticeable lack of the comprehensive solutions in the area of monitoring the vessels movement in the underwater space. Which is why, in order to increase the safety of ship traffic in the seashore, appropriate actions should be taken to recognize this technology gap.

Monitoring of the vessels traffic in the underwater space can be conducted through the use of passive underwater observation systems. They provide continuous observation and recognition of the moving objects independently of the active systems. Additionally, they do not emit any signals, which makes them undetectable for the other systems, limiting the effects of intentional dysfunction. The disadvantage of these systems is the limited range of their capabilities. This limitation is due to the actual ranges of the devices for the detection of the objects moving through the water.

Passive observation system makes it possible to acquire information about moving floating objects based on the measurement of the disturbances of local physical fields coming from the lower hemisphere. Measuring the magnitude and nature of these disturbances can constitute the complement of the available information, e.g., from the VTS system discussed above, thus supporting navigation in areas of increased vessels traffic.

Moreover, the need for the development of the passive underwater observation techniques fits in the direction of current research conducted worldwide especially since the conflict between Russia and Ukraine (Bueger and Liebetrau 2023; Voytyuk 2022).

From the point of view of the navigation safety, having information about the disturbances of individual physical fields it is possible to detect a floating object, identify it and determine the direction of its movement.

Therefore, the main goal of the first stage of the work was to determine the parameters characteristic of the analyzed hydroacoustic signature in a given water region using a passive measurement system. In order to achieve the aim of the work, it was necessary to analyze disturbances of the physical fields generated by the ship, develop a methodology for measuring hydroacoustic disturbances, and conduct a measurement experiment. In the next stages, it is planned to present the feasibility of short-range disturbance detection sensors for physical fields, i.e. magnetic, pressure and electric fields.

2. Physical fields disturbances measurements

Measurements of physical field disturbances in the underwater space are carried out in a specific area using a measuring range. The measuring range can be a complete stationary (fix) system, the individual components of which are placed in specific locations relative to each other, or the equivalent in the form of a mobile system, set up in a pre-selected location. The second solution is more flexible in terms of application on any body of water.

2.1. Measurement system description

Underwater observation of the floating objects is usually carried out using passive measurement systems. The passive measurement systems include stationary and mobile systems. Stationary systems are built based on the sensors placed permanently in specific locations in the water body. They are characterized by high accuracy. Unfortunately, such systems, due to their fixed geographical position, are easy to detect and have limited applicability. Therefore, the scope of their application for military purposes is limited. An alternative solution are mobile systems, which can be used anywhere and at any time. The constructions of the measuring platforms of the above-mentioned systems are adapted to specific depths of the water body. As a result, the possibilities of their application are limited to the selected water regions with the required depth. However, an appropriate configuration of the measurement path can provide comparable technical performance to stationary systems.

A mobile measurement system was used to measure the physical field disturbances. This system was designed and built by a team of Naval Academy employees. Currently, a comparable mobile underwater survey system is not available in Poland. Similar solutions are being developed in other countries, Germany, Spain, Sweden, Norway or the Netherlands, however, they are not available due to their military application.

The schematic diagram of the simplified measurement system prepared by the team of Polish Naval Academy is shown in Figure 1.

The mobile system for measuring physical fields of the vessels includes an integrated underwater observation module and a shore-based control module. Both these modules are connected with each other by an underwater hybrid cable.

The basis of the mobile measurement system is an integrated underwater observation module (underwater module). The integrated underwater observation module shown in Figure 2 is equipped with hardware necessary for its correct operation. The design of the integrated underwater observation module is adapted to the hydrological parameters of the destination water region. This construction enables the underwater module to be placed on the bottom in any place of the Gulf of Gdansk and in the coastal zone of the Baltic Sea. It ensures tightness during the measurements and protects the sensors together with the whole equipment against mechanical damage. The measurement sensors are mounted so that the design does not interfere with their operation.

The performance of the mobile measurement system was comprehensively tested at the laboratory tests stage. Two gel batteries are placed inside the underwater module. One is the power source for the module, the other acts as an energy buffer recharged during the operation of the underwater module by the shore-based control module. The batteries were selected based on the calculated energy balance shown in Table 1.

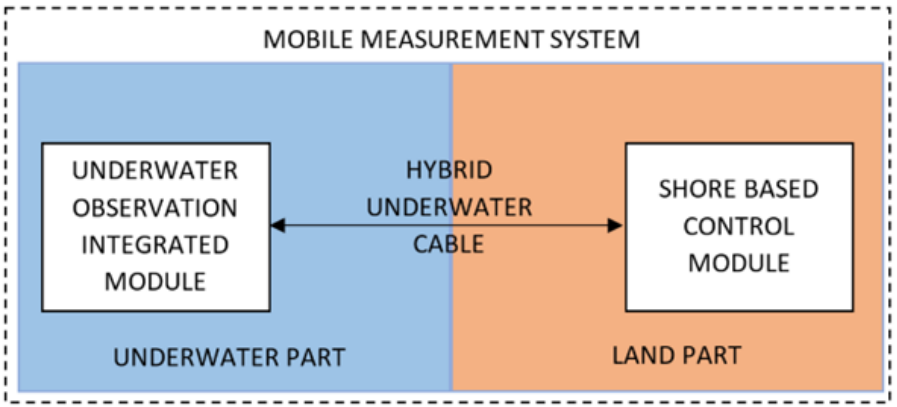

Fig. 1. Schematic diagram of the mobile physical field measurement system

Table 1. Energy balance of the integrated underwater observation module

No.	Receiver of the energy	Power consumption during standby phase [W]	Power consumption during recording phase [W]
1.	Recorder	9.60	18.00
2.	Hydrophone	0.25	0.25
3.	Magnetometer	0.00	0.36
4.	Hydrodynamic pressure sensor	0.00	0.24
5.	Gradiometer	0.00	2.60
6.	Sound velocity sounder with hydrostatic pressure sensor	0.00	0.35
7.	Inclinometer with compass	0.00	0.26
	Total	9.85	22.06

Based on the results of the presented energy balance, the capacity of the batteries located inside the underwater module was selected to be 100 Ah. This capacity of the batteries ensures the module's operation time maximum up to 50 h without charging. A rule of thumb was used to select the battery capacity for a specific supply voltage (12 VDC for this system) and the maximum current consumption of the system (< 2 A for this system), with the assumption that the capacity should be up to 10% higher than the calculated one.

The sensors located outside of the underwater module are protected from mechanical damage by a welded frame made of aluminum tubes.

The heart of the underwater module is the recorder. It is an industrial computer with a real-time operating system. The computer has an integrated circuit consisting of a Field-Programmable Gate Array (FPGA). The use of an FPGA allows the implementation of the algorithms to process signals recorded by sensors directly on the integrated circuit. The computer design is equipped with a number of input and output interfaces to which various types of sensors are connected. The built-in precision clock allows for time synchronization of signals from all measurement inputs. This results in simultaneous start of measurement on each channel, both analogue and digital. The diagram of the integrated underwater observation module is shown in Figure 3.

Set of the sensors of the integrated underwater observation module is adapted to the requirements and assumptions of the mobile measurement system. The ranges of the measured physical quantities were selected to match the environmental parameters of the Baltic Sea and other water regions with depths up to 100 m. The first sensor described is the Reson TC-4032 hydrophone with high sensitivity used to measure the hydroacoustic field. The selected sensors meet the assumptions in terms of hydrophone voltage sensitivity (> -170 dB re 1 V/μPa) and resistance to conditions for depths above 100 m. The hydrophones belong to the measuring class of equipment, which also includes Bruel & Kjaer sensors, which are much more expensive, why the Reson product was chosen.

The Reson TC-4032 hydrophone has a flat frequency response over a wide bandwidth. The frequency bandwidth of the hydrophone is from 5 Hz to 120 kHz. The linear frequency range is within the range of 15 Hz to 40 kHz with a maximum deviation of ±2 dB and within the range of 10 Hz to 80 kHz with a deviation of ±2.5 dB. The Reson TC-4032 hydrophone is powered by 12 VDC. The analogue output signal of the hydrophone is differentially connected to the underwater measurement module, which provides this way receiving efficiency of -164 dB re 1V/μPa. The described hydrophone is characterized by an omnidirectional horizontal directional characteristic and a vertical directional characteristic of 270°. The hydrophone uses a preamplifier with a gain of 10 dB, which enables the recording of a low-level signal corresponding to the zero state of the sea. This feature allows us to record and later extract useful signals which are in the background of an ambient noise.

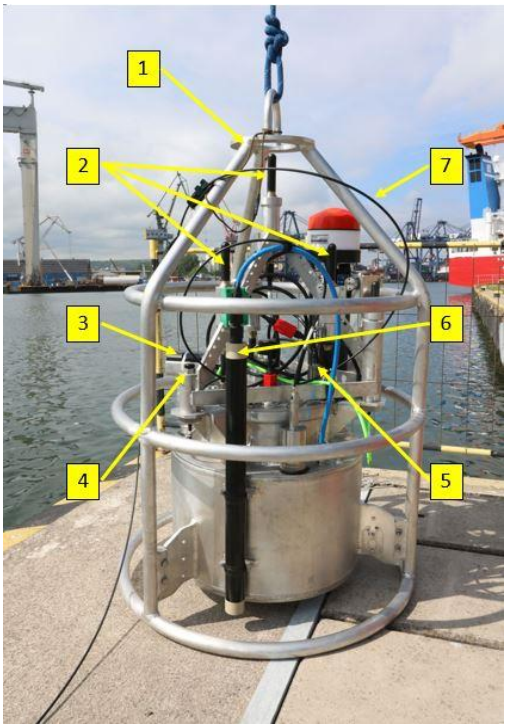

Fig. 2. Integrated underwater observation module with listed components: (1 – aluminum frame, 2 – hydrophones, 3 – magnetometer and inclinometer with compass in one housing, 4 – hydrodynamic pressure sensor, 5 – sound velocity sounder with hydrostatic pressure sensor, 6 – gradiometer, 7 – underwater hybrid cable

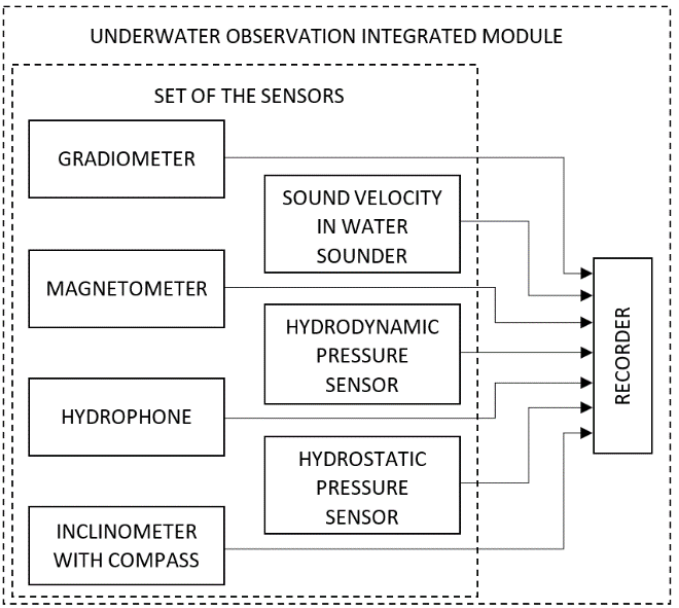

Fig. 3. Diagram of the integrated underwater observation module

The integrated underwater module was equipped with the sensors shown in the block diagram of Figure 3. Due to the hydroacoustic field analyses and the possibility as an application to classify the measured vessels, the data from the other sensors will not be discussed in this paper. Information obtained from the sensors described above is supplemented with data from auxiliary sensors. An inclinometer with a compass Honeywell HMR3300 was used to measure the tilt and the position of the underwater measuring module relative to the North.

The described sensor has a built-in RS-232 serial interface for digital communication and data exchange. Direction relative to North is measured by means of a built-in compass within the range from 0 to 360˚, with resolution of 0.1˚ and accuracy of 1˚. Inclinometer is responsible for the measurement of a tilt in the range between -60 to 60˚. The measurement is carried out with a resolution of 0.1˚ and an accuracy of 0.4˚ in the range between -30 to 30˚ and 1˚ in the range between -60 to -30˚ and between 30 to 60˚.

Another auxiliary tool of the measurement system is a sounder to measure the velocity of sound in water. Information about the velocity of sound in water is important for measuring the hydroacoustic field in the water regions with varying salinity and water temperature because of the effects of salinity, temperature, and pressure on the velocity of sound propagation Valeport mini SVS sounder was used for direct measure of sound velocity in the water.

The velocity of sound is being done by measuring the pulse transit time between the transmitter and receiver, which are at a fixed distance from each other. The sounder has a built-in RS-485 serial interface for digital communication. The sounder can measure the velocity of sound in the range between 1375 to 1900 m/s, with a resolution of 0.001 m/s and an accuracy of ±0.02 m/s.

The last of the auxiliary sensors used is the hydrostatic pressure sensor which used for the measuring the depth at which the underwater module is located. This sensor is located in the housing of the sound velocity sounder. The hydrostatic pressure value is sent to the recorder via RS-485 serial interface. Hydrostatic pressure measurement is carried out in the range up to 10 Mpa. The measurement resolution is 10 Pa and the accuracy is 20 Pa.

All of the sensors mentioned above are connected to a computer enclosed in a sealed capsule which records the received signals. They constitute the underwater module of the mobile measurement system.

The operation of this module is managed by the shore-based control module, the diagram of which is shown in Figure 4.

The shore-based control module provides adequate power supply to the integrated underwater observation module and communication between the underwater and shore-based parts of the measurement system. The shore-based control module allows recording of the measured physical fields on the non-volatile memory. An additional function of the module is to preview the values of the currently measured physical quantities. The shore-based control module consists of:

– Communication and power supply assembly,
– Operator panel.

The communication and power assembly is an intermediate element between the underwater observation module and the operator panel. The communication and power supply assembly consists of: programmable DC power supply, set of batteries with pulse charger, Ethernet switch and optical-Ethernet converter. Such built assembly provides two-way communication between the underwater and shore-based parts of the measurement system. The second function of the shore-based control module is to turn on the power to the underwater module and to charge the batteries inside the underwater module. The batteries are charged via an underwater hybrid cable. The charging process is controlled by a programmable DC power supply. The power supply is located inside the communication and power assembly.

It also contains a set of batteries enabling operation of the underwater module without external power supply. The control of the communication and power supply assembly is performed from the operator panel.

The operator panel is a Dell OptiPlex computer with software for complex control of the measuring system operation. The software installed on the computer is responsible for management of the measurement process and control of power supply to the underwater module. The whole system works simultaneously ensuring the consistency of the measurement process.

An important element necessary for the operation of the mobile measurement system is an underwater hybrid cable. For the measurements was used a 1 km long cable, consisting of four optical fibers protected by a stainless-steel tube and a copper-steel braid. The tube together with the braid acts as power supply cables for the underwater module separated by insulation. The described cable construction ensures trouble-free communication between the underwater module and the shore-based control module.

The mobile measurement system presented above was used to study the physical fields of vessels navigating in the Gulf of Gdansk area.

2.2. Description of the measurements conducting methodology

Conducting of the measurements of the physical fields of the vessels required the development of an appropriate methodology. It involved the preparation phase of measuring equipment, during which the measurement system was calibrated. Then the survey area was to be planned, the location for the placement of the measuring system on the bottom of the basin was to be selected, and the routes of passage of vessels and their speed were to be developed. After conclusion of the preliminary activities, it was possible to proceed to the recording of the parameters of selected physical fields of the ship. The last step of the methodology was the development and analysis of the obtained measurement results.

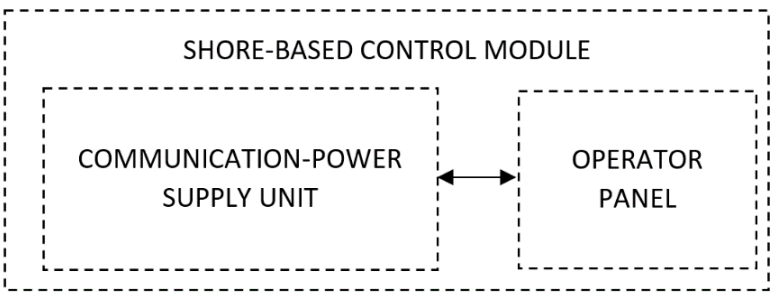

Fig. 4. Diagram of the shore-based control module

2.2.1. Measurement system calibration

The calibration process of the measurement system included a complete measurement path for sound pressure. For this purpose, the integrated underwater observation module was connected, via an underwater hybrid cable, to the shore-based control module. During first step, the measurement sensors had to be calibrated. To calibrate the hydrophone, a vibration exciter was used which, when placed on the hydrophone, generated an acoustic pressure of constant frequency and amplitude values specified in the exciter's catalogue note. Based on this value, the pressure value recorded by the measuring system was recalculated. The resulting correction was entered into the software. After calibration, the measurement system was ready to perform measurements in actual conditions.

2.2.2. Setup of the measuring system on the bottom of the water body

Before starting the measurements in actual conditions, the elements of the measuring system had to be transported to the predetermined geographical positions using small hybrid boat.

Before lowering the underwater module, the underwater connector of the hybrid cable located on the reel was connected to the module. Then the module was deployed on the bottom at 20 m depth and its geographical position was recorded using a handheld GPS receiver. Once the geographic position of the underwater module was determined, the hybrid boat was moved to the base vessel where the shore-based control module was placed. As the boat was being moved, the underwater hybrid cable was unwound from the reel. The length of used cable was 1 km. Upon reaching the anchored base vessel, the reel with the underwater hybrid cable was transferred to the deck of the unit. The cable was then connected to the communication and power unit of the shore-based control unit. During the first start-up of the measuring system, the value of the tilt angles of the underwater module is recorded and its tightness is verified by means of water level sensors placed inside the module.

In the next phase of preparation, the geographical position and the position of the module is verified. For this purpose, a diver was transported to the position recorded during lowering of the integrated underwater observation module. The diver's task was to correct the position of the module according to the geographical North. After the correction was made, the final geographical position of the module was recorded with DGPS correction accuracy.

2.2.3. Conducting of the measurements of the physical fields of the vessels

Measurements of the physical field disturbances caused by the vessels in real conditions were carried out for two types of objects. The first of them was a buoy tender and an ocean-going tugboat. The vessels were moving according to a predetermined plan, i.e., with a given speed and heading. During the individual passes, the motion parameters and the geographical position were obtained from the on-board satellite navigation system were recorded.

The vessels passed at different distances from the position of the underwater module in order to obtain spatial distributions of the disturbances of the tested physical fields.

The second type of floating objects were random vessels entering and leaving the Gdynia harbor. The vessels were moving at different times, therefore, continuous observation of the situation in the area of the Gulf of Gdansk was required. For this purpose, an additional on-board AIS system located on the base vessel was used. Uninterrupted observation at the electronic chart was conducted by a person who simultaneously provided information about the beginning and the end of the measurement. Each measurement started when the vessel crossed the line marked on the map, located 400 m before the geographical position of the underwater observation integrated module. The measurement was finished when the observed vessel crossed the line marked on the map, which was 400 m behind the geographical position of the underwater observation integrated module.

Recording of the measurement data was conducted during the passage of the object in the area where the underwater observation integrated module was placed according to the diagram shown in Figure 5. The movement of the vessel for which the physical fields were measured was in the East-West direction and vice versa. According to the previous assumptions, the results of the hydroacoustic field measurement were analyzed in detail. During real tests this field was measured continuously. It means that uninterrupted watch with the use of the hydrophone was conducted. Such an approach to tests was necessary to determine the level of background noise,

which is variable in the real water environment. Knowledge of the noise value variations is the basis for determining the average background noise level L_t [dB re 1 µPa]. The value L_t was calculated from the relation as follows:

$$L_t = \sqrt{\frac{1}{N}\sum_{n=1}^{N}|X_n|^2} \quad (1)$$

where:
L_t is the RMS value of the hydroacoustic ambient signal occurring in the measurement window from N the samples corresponding to the signal duration time which is equal to 5 min,
X_n is the hydroacoustic ambient signal.
This value is required for further analysis of the floating object hydroacoustic data. The average background noise level of the water body L_t was determined 5 minutes prior to the start of the measurement in frequency range from 3 Hz to 25 kHz, which was determined by frequency sampling of ADC. This allowed us to determine the actual conditions in the area during the measurements.
Analysis of hydroacoustic data of a floating object was performed for the time when the level of sound pressure exceeded the value L_t+10 dB re 1 µPa. The value 10 dB re 1 µPa was determined on the basis of long-term analyses for the background noise in the Gulf of Gdansk region.

3. Results of the hydroacoustic field measurements

This caption presents the results of hydroacoustic field measurements in the form of SPL (Sound Pressure Level). SPL curves for different vessels and for different moving speeds of the same vessel are compared. In the following section, an algorithm to track the moving sound source is presented. In the final part of the chapter are shown parameters describing the SPL curve used in the ship classification process. Disturbances of the hydroacoustic field caused by a vessel were analyzed in the time domain. The results of the sound pressure measurements for the selected vessel were related to the actual geographical position of the underwater module while simultaneously taking into account the vessel speed. This way, spatial distribution of sound pressure level changes was obtained, which is shown in Figure 6.
The spatial distribution of sound pressure level changes shown in the figure above is the result of noise measurements from a vessel moving in the North direction. The area for which the distribution is colored in red corresponds to the highest value of the sound pressure level, i.e., 152 dB re 1 µPa. This level decreases to the value below 120 dB re 1 µPa as the distance of the moving vessel from the underwater module increases.

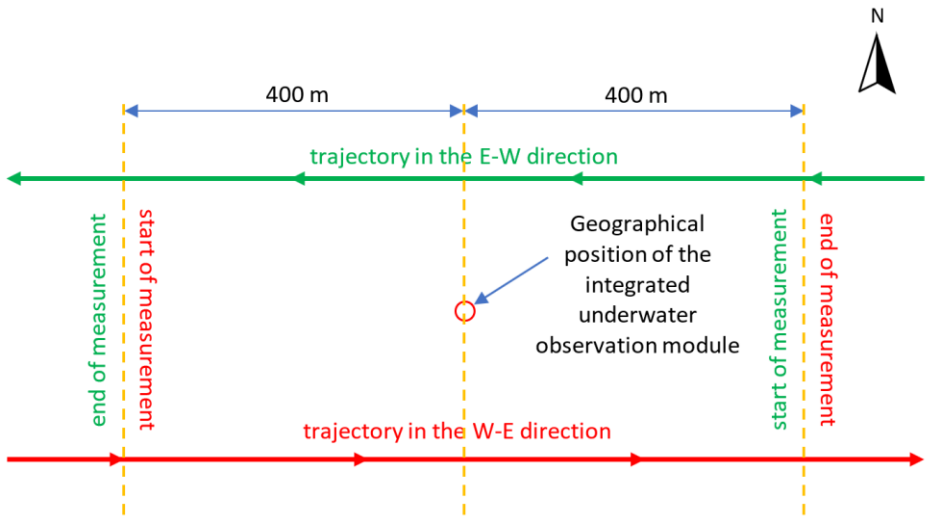

Fig. 5. Diagram of the start and the end of the measurement

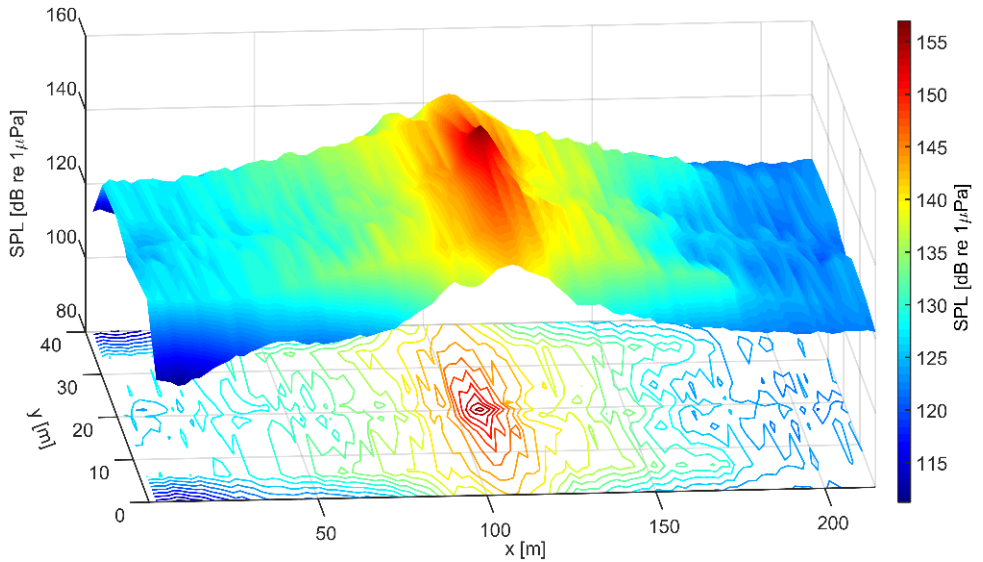

Fig. 6. Example of the spatial distribution of sound pressure level induced by the passing vessel

In the further part of the analysis of the conducted research, the change of the sound pressure level for the selected vessels is presented (Buszman, Gloza 2020). The fairway along which the surveyed objects moved was about 30 m away from the geographical position of the underwater measuring module. Whereas, the speed of the vessels was constant and it was about 8 m/s. The results of the recorded measurements are shown in Figure 7.

Figure 7 shows a summary of the curves of sound pressure level changes over time for 3 different vessels. These vessels were moving with the same speed and course and the same distance to the measuring system. The background noise level were comparable. The highest average sound pressure level was recorded for the Ro-Ro vessel. In comparison, the smallest noise was generated by the passenger ferry, which is the smallest of the vessels tested. Whereas, the sound pressure distribution for the buoy tender showed the highest dynamics of change of the examined parameter in time. It means that the value of sound pressure increases rapidly when the object approaches the geographical position of the underwater measuring module and decreases rapidly when it moves away from the measuring position. The analysis of changes in the sound pressure level curve showed that its shape depends on the type of vessel. The time for which the tested vessels passed closest to the geographic position of the underwater measuring module corresponds to the time of eight-ieth-eighth second on the time line in Figure 7.

Due to the nature of the hydroacoustic field and the water environment, sound propagation is accomplished by transmitting vibrations from the source to the water in which the underwater portion of the hull is located. The main source of noise on a vessel is the ship's equipment mounted inside. An example diagram of such equipment is shown in Figure 8. The hydroacoustic disturbance is generated by the working propulsion system and by the noise associated with the flow of water around the hull. During operation, the propulsion system generates hull vibrations of various frequencies. These vibrations result primarily from the rotational speed of individual marine machines and devices (Łosiewicz at al., 2022). In addition, the ship's hull moving in the water generates noise caused by the turbulent flow of water around the hull.

The value of these vibrations influences the level of generated sound pressure and the range of propagated elastic wave (Klusek at al., 2015). The knowledge of the characteristic frequency components for a given type of ship and her working machinery provides the required information about their source. This knowledge allows us to develop the acoustic characteristics of a given type of the

ship, which can be used to determine the direction of her movement. Knowledge of the acoustic characteristics of individual types of ships allows them to be identified, tracked and thus affects the safety of maritime transport.

In the next step, the effect of vessel speed on the level of generated underwater noise is presented. For this purpose, sound pressure measurements were conducted for 3 different speeds of a selected type of the vessel. The distances of the vessel transitions from the geographical position of the underwater module were less than 10 m. In order to compare the effect of vessel speed on the sound pressure level, a summary of the results is presented in Figure 9.

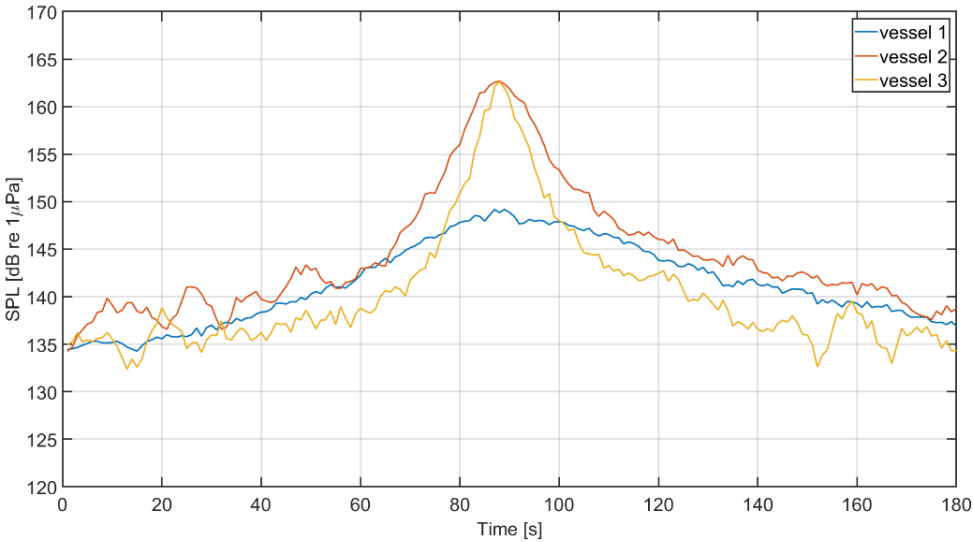

Fig. 7. Summary of sound pressure level results for different types of vessels (vessel 1 – 37 m long passenger ferry, vessel 2 – 160 m long Ro-Ro vessel, vessel 3 – 60 m long buoy tender)

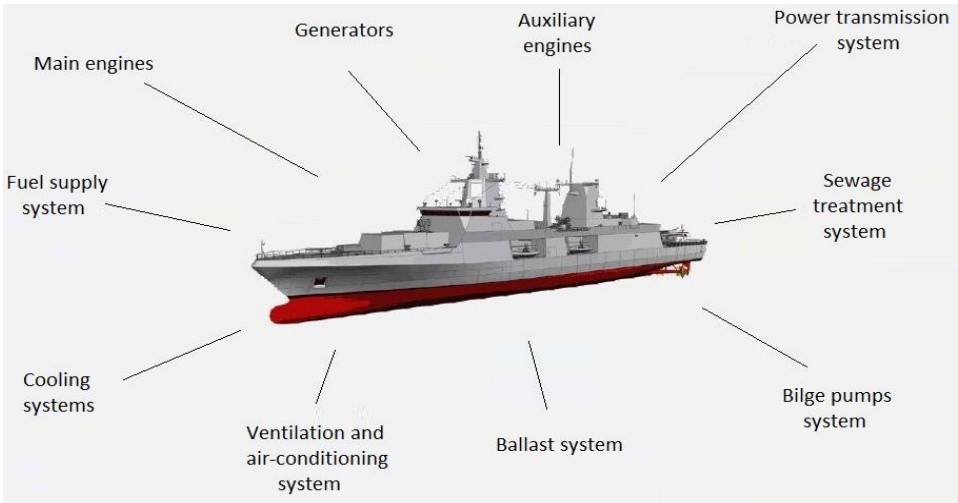

Fig. 8. Diagram of vibration and noise sources of the exemplary vessel

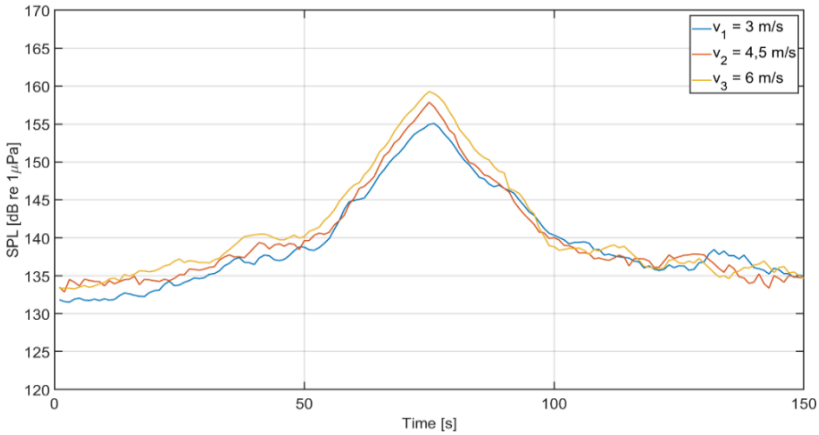

Fig. 9. Summary of the sound pressure level results at different speeds (v_1 = 3 m/s, v_2 = 4,5 m/s and v_3 = 6 m/s) for the same object

From the sound pressure variation curves shown in Figure 9, it is evident that the sound pressure level increases as the vessel speed increases. The nature of the changes shows similarity for all three speeds. It is observed that for 2 times increase in speed (from 3 m/s to 6 m/s), the maximum sound pressure level increased by 4 dB re 1 μPa. This means that as the vessel speed increases, the sound pressure value increases.

The movement of the vessel is the result of the propulsion system operation, whose parameters directly affect the speed of the vessel. An increase in the vessel's speed is the result of an increase in the rotational speed of the individual machinery which constitutes propulsion system. As a result, the overall noise and vibration level of the vessel increases, which consequently corresponds to an increase in the sound pressure measured at a certain distance from the source.

Analyzing the data presented in the above graphs, the dependence of the shape of the curve of sound pressure changes in time on the type of the tested vessel (Figure 7) and on the motion parameters of the selected vessel (Figure 9) is clearly visible. The course of changes in the sound pressure level depends on the parameters which are related to the size and shape of the object, and the speed of the object movement. Detailed analysis of the above graphs and many others obtained during the research will allow to describe the changes of sound pressure values in time by means of a set of parameters, the selection of which is described in the following part.

3.1. Tracking of a moving object

Tracking of a floating object was realized using analysis of signals from 4 hydrophones in tetrahedral configuration (Gloza at al., 2013; Buszman 2018). Hydrophones were placed on the tetrahedron vertices with a distance of 0.25 m between sensors. The positions of the 6 virtual hydrophones were geometrically determined at the centres of each tetrahedron edge. Connecting the centre of the edge on which the selected hydrophone pair was located to the centre of the edge for the remaining pair obtained one of the 3 axes of the Cartesian coordinate system. Performing the operation for the remaining 2 combinations of hydrophone pairs resulted in a complete Cartesian coordinate system, what is presented in Figure 10.

The X axis is determined by the virtual hydrophones V2 and V4, where the signal V2 takes the mean value of the hydrophone signals H2 and H3. The V4 signal was determined from the signals of hydrophones H1 and H4. Y axis is determined by virtual hydrophones V5 and V6. Signal V5 takes the average of the signals from hydrophones H1 and H3, and signal V6 takes the average of the signals from hydrophones H2 and H4. The Z axis is determined by virtual hydrophones V1 and V3. Signal V1 takes the average of the signals from hydrophones H1 and H2, and signal V3 takes the average of the signals from hydrophones H3 and H4.

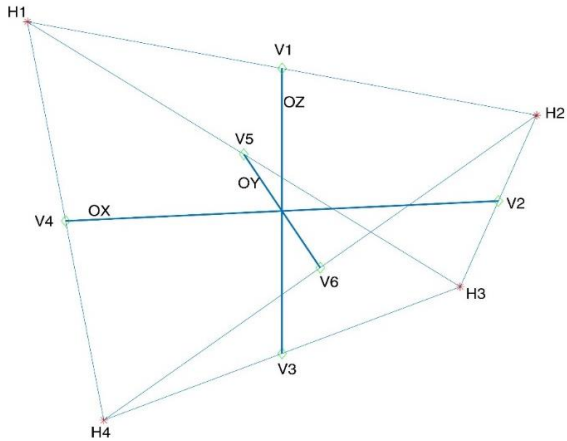

Fig. 10. Tetrahedral configuration of hydrophones (H1 – H4) with virtual points (V1 – V6)

To determine the signal for the selected virtual sensor, the time delay between the signals for the corresponding pair of hydrophones was determined. For signal V1, the autocorrelation function of the signal from sensor H1 was determined according to the formulas as follows (Gloza at al., 2013):

$$R_{H1}(\tau) = \int_{-\infty}^{\infty} H1(t) * H1(t-\tau)dt \tag{2}$$

In the next step, the cross-correlation function of the signals from H1 and H2 sensors was determined based on the relation (Gloza at al. 2013):

$$R_{H1H2}(\tau) = \int_{-\infty}^{\infty} H1(t) * H2(t-\tau)dt \tag{3}$$

Based on the obtained results, the maximum of the autocorrelation and cross-correlation functions is found. The delay τ is determined, based on which the signal from the sensor H2 is shifted in phase with the signal from the sensor H1.

$$H2'(t) = H2(t \pm \tau) \tag{4}$$

The resultant signal is determined according to the formula:

$$V1'(t) = \frac{H1(t)+H2'(t)}{2} \tag{5}$$

Finally obtaining the signal after the phase shift:

$$V1(t) = V1'^{\left(t \mp \frac{\tau}{2}\right)} \tag{6}$$

The x, y and z components of the sound intensity were calculated from the following equations (Fahy 1995; Gloza 2002):

$$Ix = -\frac{Im\{G_{V4V2}\}}{2\rho\omega x} \tag{7}$$

$$Iy = -\frac{Im\{G_{V5V6}\}}{2\rho\omega x} \tag{8}$$

$$Iz = -\frac{Im\{G_{V1V3}\}}{2\rho\omega x} \tag{9}$$

where:
ρ is water density,
ω = 2πf is pulsation of the analyzed signal,
$2x = d/2^{1/2}$ is the distance between virtual hydrophones,
$Im\{G_{VAVB}\}$ *is* the cross spectrum imaginary part.
Knowing the intensity components *Ix*, *Iy* and *Iz* it was possible to determine the bearing on the noise source according to the formulas (Gloza at al., 2013):

$$\varphi = \arctan\left(\frac{Iy}{Ix}\right) \tag{10}$$

$$\theta = \arccos\left(\frac{Iz}{I}\right) \tag{11}$$

where:

$$I = \sqrt{Ix^2 + Iy^2 + Iz^2} \tag{12}$$

Based on the instantaneous position of the moving object in space and the change of position in time, it

is possible to determine the parameters in the time domain. Additionally, it is possible to determine the speed of the analysed object.

3.2. Selection of hydroacoustic field parameters with respect to the time domain

Parameters related to the shape of the sound pressure level change curve are used to describe the hydroacoustic field (Buszman 2016). The selected parameters in the time domain are shown in Figure 11.

The first parameter chosen to describe the hydroacoustic field is the duration of the disturbance t [s]. This is the time calculated from the moment when the average background noise level L_t is exceeded by 10 dB re 1 μPa until the measured sound pressure level decreases to L_t+10 dB re 1 μPa.

The next selected parameter is the maximum level of the sound pressure L_{max} [dB re 1 μPa]. It is determined for the interval of one second duration during which the tested source generated the largest disturbance. The value of this parameter was determined from the relation for the effective value of the RMS signal (Root Mean Square):

$$U_{RMS} = \sqrt{\frac{1}{N}\sum_{n=1}^{N}|X_n|^2} \tag{13}$$

where:

U_{RMS} is the RMS value of the hydroacoustic signal occurring in the measurement window from N the samples corresponding to the signal duration time which is equal to 1 s,

X_n is the hydroacoustic signal analysed.

The next parameter is t_{max} [s] designating the time for which the interference source generated the highest level of sound pressure described by the maximum signal level L_{max}. This time is measured from the moment of crossing the threshold of the average background noise level by 10 dB re 1 μPa.

The last parameter is the area of the figure bounded by the curve of the averaged sound pressure level and a line representing the average background noise level augmented by 10 dB re 1 μPa marked by the symbol S_p [(dB re 1 μPa)·s].

3.3. Methodology for analyzing measurement results

The parameters presented in the previous section were analyzed to search for correlations between them and their sources in the form of vessels. One of the K-NN (K - Nearest Neighbors) classification methods was used, which uses the Euclidean distances between individual results on the x-y plane. In order to obtain suitable input data for this method, selected parameters were normalized according to the relation (Horzyk A. and Starzyk J. A. 2019):

$$x_i' = \frac{x_i - x_{min}}{x_{max} - x_{min}} \tag{14}$$

where:

x_i' – resulting parameter value after normalization,

x_i – value of the tested parameter,

x_{min} – the smallest value of the parameter of all tested objects,

x_{max} – the highest value of the parameter of all tested objects.

The normalization resulted in SpN, LmaxN, tmaxN and tN, corresponding to the parameters shown in Figure 11.

During the measurements, dozens of ship transitions were recorded and grouped as follows:

- S1 – dedicated vessel 1 moving at a short distance from the measurement module (up to 10 m),
- S1-1 – dedicated vessel 1 moving at a greater distance from the measurement module (further than 15 m),
- S2 – dedicated vessel 2 moving at a short distance from the measurement module (up to 20 m),
- S2-1 – dedicated vessel 2 moving at a greater distance from the measurement module (further than 25 m),
- S3 – passenger ferries with a value of GT > 20000,
- S4 – container ships with a value of GT > 10000.

The normalized parameters were placed in pairs on a common plane with grouping. The pair S_pN and $L_{max}N$ is shown in figure 12, and the pair $t_{max}N$ and tN is shown in figure 13.

Comparing the figures, one can observe a clustering of results for the first pair of parameters (S_pN and $L_{max}N$), as opposed to the other pair ($t_{max}N$ and tN). The analysis for the other 4 pairs was carried out in a similar manner, i.e.:$L_{max}N$ with tN, $L_{max}N$ with $t_{max}N$, S_pN with tN i S_pN with $t_{max}N$.

The next step was to determine the Euclidean distance for the extreme points of each set. The value

of the Euclidean distance determines the degree of clustering of the elements of the set. This value decreases as the clustering of the elements of the set increases. To determine the Euclidean distance, the relationship shown below was used:

$$d(x,y) = \sqrt{(x_{max} - x_{min})^2 + (y_{max} - y_{min})^2} \quad (13)$$

where:
x_{min} i x_{max} – the smallest and largest parameter value of a given set of elements represented by the x-coordinate,
y_{min} i y_{max} – the smallest and largest value of the second parameter of the same set of elements represented by the y-coordinate.
The average value of the Euclidean distances of each combination of parameter pairs was determined. The results obtained are presented in the form of a colored matrix (figure 14).
The fields with the darkest color correspond to the smallest Euclidean distances, i.e. the largest clustering of the collection. Based on the above analysis, a pair of hydroacoustic field parameters was selected S_pN and $L_{max}N$, showing the highest concentration of the set of elements.

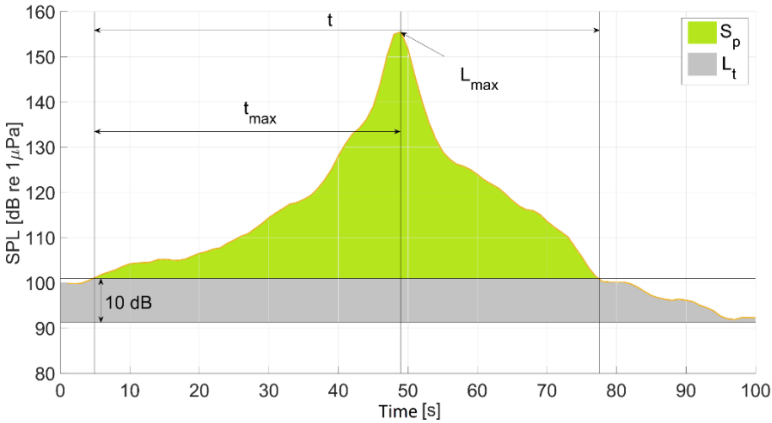

Fig. 11. Parameters related to the hydroacoustic pressure level

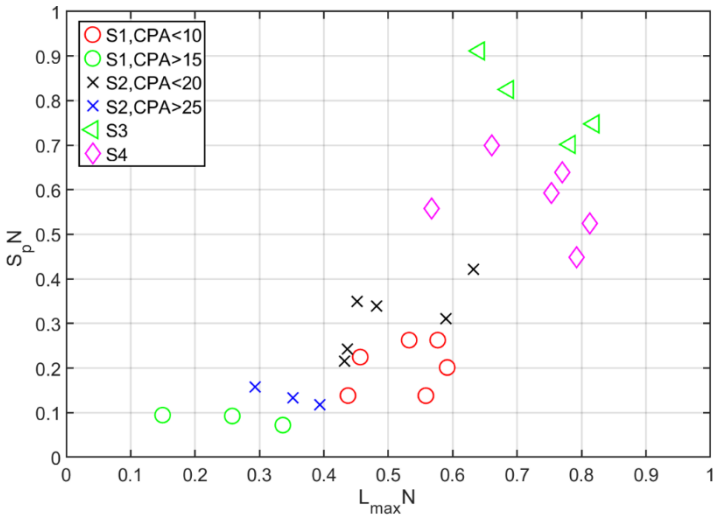

Fig. 12. Representation of normalized parameter pairs S_pN i $L_{max}N$

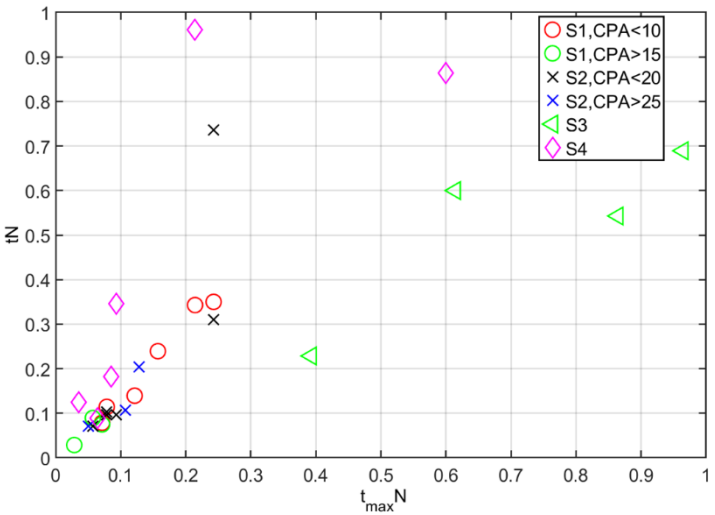

Fig. 13. Representation of normalized parameter pairs tN i $t_{max}N$

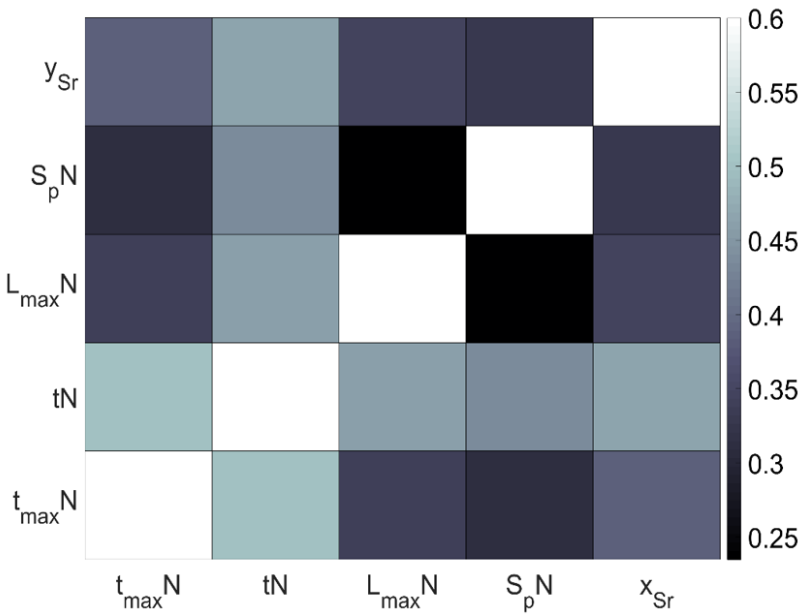

Fig. 14. Color matrix of average values of Euclidean distances

The parameters described above can be used to parametrize the hydroacoustic field what will be the next phase of research. Based on these parameters, it will be possible to carry out a classification of vessels taking into account their speed and distance from the geographical position of the underwater module. In addition, long-term underwater situation surveillance will allow the development of a database of the vessels operating in a given location along with the determination of the characteristics of

the noise they generate. This aspect can be used for critical infrastructure protection as well as for noise monitoring in a selected water region. Underwater observation of the movement of vessels in a given sea area will additionally increase the safety of maritime transport.

4. Discussion

The analysis of research on disturbances in the hydrostatic field caused by floating objects using an underwater measurement module, carried out in the article, provided the basis for justifying the need to extend the monitoring of ship traffic to the lower hemisphere. A review of available systems supporting the navigation process indicated a clear technological gap in the field of underwater observation. The information obtained about the physical signature of ships, and in particular about the hydroacoustic field, increases the possibilities of monitoring ship traffic in the area of strategic infrastructure facilities. Additional data about ships generating underwater noise may supplement, and in some cases even replace, data recorded by subsystems included in the currently operating maritime traffic safety system VTS.

Presented method of conducting measurements of physical fields of the vessels demonstrated the possibility of using a mobile measurement system for this purpose. The mobile measurement system developed by the Naval Academy in the presented configuration can be used in any water region where depth does not exceed 50 m. The indicated areas concern the offshore zone and harbor approach fairways.

The presented research results and analysis of measurements of hydroacoustic field disturbances carried out in real navigation conditions showed the distinguishability of vessels (i.e. type, application) with various motion parameters based on the size and shape of the noises recorded by the measurement system. It was also checked whether there is a relationship between the level of noise generated and the speed of movement of a given ship. Dedicated ships used for this purpose facilitated the development of a method for parameterizing hydroacoustic field disturbances.

By examining the possibilities of analyzing signals obtained from individual sensors measuring disturbances in the hydroacoustic field, some parameters in the time domain were obtained. For this reason, qualitative and quantitative verification of individual parameters was required. For this purpose, a parameter selection method was developed using the values of Euclidean distances between individual pairs of parameters. In order to conduct an analysis verifying the parameters in terms of determining their quality, normalization was used. The normalization of physical quantities, taking values from various ranges and physical units, made it possible to present every possible combination of pairs of parameters on the plane. The use of a two-stage analysis of pairs of normalized parameters allowed for the determination of parameter selection criteria.

These data can serve as a basis for the movement of vessels in the analyzed area and directly increase the level of navigation and maritime safety in the sea area of strategic infrastructures.

References

[1] Aman, W., Al-Kuwari, S., Kumar, A., Ur Rahman, M. M., Muzzammil, M. (2022) Underwater and Air-Water Wireless Communication: State-of-the-art, Channel Characteristics, Security, and Open Problems. arXiv:2203.02667v2,2022. https://doi.org/10.48550/arXiv.2203.02667.

[2] Aman, W., Al-Kuwari, S., Muzzammil, M., Ur Rahman, M. M., Kumar, A. (2023). Security of underwater and air–water wireless communication: State-of-the-art, challenges and outlook. Ad Hoc Networks, 142, 103114. https://doi.org/10.1016/j.adhoc.2023.103114.

[3] Blanchard, C., Harrould-Kolieb, E., Jones, E., Taylor, M. L. (2023). The current status of deep-sea mining governance at the International Seabed Authority. Marine Policy, 147, 105396. https://doi.org/10.1016/j.marpol.2022.105396.

[4] Blok, M. et al. (2018). Streaming Real-time Data in Distributed Dispatcher and Teleinformation Systems for Visualization of Multi-media Data of the Border Guard. Trans Nav: International Journal on Marine Navigation and Safety of Sea Transportation, 12 (2), 217-229. https://doi.org/10.12716/1001.12.02.0.

[5] Bueger, C., Liebetrau, T. (2023). Critical maritime infrastructure protection: What's the trouble?. Marine policy, 155: 10577. https://doi.org/10.1016/j.marpol.2023.105772.

[6] Buszman, K. (2013). Examination of acoustic wave propagation in real conditions. Hydroacoustics, 16, 11-18.
[7] Buszman, K. (2016). Signals parametrization method of sailing vessels. Hydroacoustics, 19, 27-36.
[8] Buszman, K. (2018). Bearing Calculation Accuracy for a Simulated Noise Source Using a Hydroacoustic Tetrahedral Antenna. Joint Conference - Acoustics, 1-4. https://doi.org/10.1109/ACOUSTICS.2018.8502267.
[9] Buszman, K., Gloza, M. (2020). Detection of floating objects based on hydroacoustic and hydrodynamic pressure measurements in the coastal zone. Polish Maritime Research, 27 (2), 168-175. https://doi.org/10.1016/10.2478/pomr-2020-0038.
[10] Danzell, O. E., Mauslein, J. A., & Avelar, J. D. (2023). Managing Threats on the High Seas: The Role of Naval Bases on Reducing Maritime Piracy. Armed Forces & Society, 49(1), 179–200. https://doi.org/10.1177/0095327X211049462.
[11] De Bièvre, A. (1985). Vessel Traffic Services and the Law. Journal of Navigation, 38(3), 347-364. https://doi.org/10.1017/S0373463300032720.
[12] Delgado, J., Amorim, A., Gouveia, L., Gouveia, N. (2018). An Atlantic journey: The distribution and fishing pattern of the Madeira deep sea fishery. Regional Studies in Marine Science, 23. https://doi.org/10.1016/j.rsma.2018.05.001.
[13] Dolgikh, G. I., Budrin, S. S., Dolgikh, S. G., Ovcharenko, V. V., Chupin, V. A., Yakovenko, S. V. (2017). Particulars of a transmitted acoustic signal at the shelf of decreasing depth. The Journal of the Acoustical Society of America, 142(4), 1990-1996. https://doi.org/10.1121/1.5006904.
[14] Esteban, M.D., López-Gutiérrez, J.S., Negro, V. (2020). Offshore Wind Farms. Journal of Marine Science and Engineering, 8(2), 120. https://doi.org/10.3390/jmse8020120.
[15] Fahy, F.J. 1995. Sound intensity, E&FN spon, London, 2nd ed.
[16] Fiuk, J., Chamier-Gliszczyński, N., Jacyna, M., Izdebski, M. (2022). Energy Efficiency of Transport Tasks Performed by the Air SAR System in the Baltic Sea. Case Study. Energies, 15(2), 643, 1-17. https://doi.org/10.3390/en15020643.
[17] Gloza I. (2002). Tracking the underwater noise source using a vector sound-intensity probe. Acta Acustica united with Acustica, 88 (5), 670-673(4).
[18] Gloza, I., Buszman, K., Józwiak, R. (2013). Tracking underwater noise sources with the use of a passive method. Acta Physica Polonica A, 123 (6), 1090-1093. https://doi.org/10.12693/aphyspola.123.1090.
[19] Gucma, L., Marcjan, K. (2012). Examination of ships passing distances distribution in the coastal waters in order to build a ship probabilistic domain. Scientific Journals Maritime University of Szczecin, 32(104), 34–40.
[20] Jacyna, M., Wasiak, M., Lewczuk, K., Karoń, G. (2017). Noise and environmental pollution from transport: decisive problems in developing ecologically efficient transport systems. Journal of Vibroengineering, 19 (7), 5639-5655. https://doi.org/10.21595/jve.2017.19371.
[21] Jeong, S., Ban, S. W., Choi, S., Lee, D., Lee, M. (2012). Surface Ship-Wake Detection Using Active Sonar and One-Class Support Vector Machine, IEEE Journal of Oceanic Engineering, 37(3), 456-466. https://doi.org/10.1109/JOE.2012.2192344.
[22] Kazimierski, W., Zaniewicz, G., Hyła, T. (2017). Implementation of Voyage Assistant Module in Mobile Navigation System for Inland Waters. TransNav: International Journal on Marine Navigation and Safety of Sea Transportation, 11 (4), 683-689. https://doi.org/10.12716/1001.11.04.15.
[23] Klabučar, B., Sedlar, D.K., Smajla, I. (2020). Analysis of blue energy production using natural gas infrastructure: Case study for the Northern Adriatic. Renewable Energy, 156, 677-688. https://doi.org/10.1016/j.renene.2020.04.082.
[24] Klusek, Z., Szczucka, J., Mróz, D. (2015). Selected Characteristics of Shipping Noise at the Fairway of the Gdynia Harbour. Hydroacoustics, 18, 203-214.
[25] Kong, W., Liu, S., Xu, M., Yasir, M., Wang, D., Liu, W. (2023) Lightweight algorithm for

multi-scale ship detection based on high-resolution SAR images. International Journal of Remote Sensing, 44(4), 1390-1415. https://doi.org/10.1080/01431161.2023.2182652.

[26] Kozaczka, E. (2013). Propagation of Acoustic Disturbances in Shallow Sea. Collection of acoustics and ultrasound / hydroacoustics of shallow water, 31-52.

[27] Leonart, J. (2008). Review of the state of Mediterranean and Black Sea fishery resources. Options Méditerranéennes: Série B. Etudes et Recherches, 62, 57-69.

[28] Li, L., Yu, J., Chen, F. (2022). TISD: A Three Bands Thermal Infrared Dataset for All Day Ship Detection in Spaceborne Imagery. Remote Sensing, 14, 5297. https://doi.org/10.3390/rs14215297.

[29] Loran, T., Cardoso da Silva, A. B., Joshi, S. K., Baumgartner, S. V., Krieger, G. (2023). Ship Detection Based on Faster R-CNN Using Range-Compressed Airborne Radar Data. IEEE Geoscience and Remote Sensing Letters, 20, 1-5, 3500205. https://doi.org/10.1109/LGRS.2022.3229141.

[30] Łosiewicz, Z., Mironiuk, W., Cioch, W., Sendek-Matysiak, E., & Homik, W. (2022). Application of Generator-Electric Motor System for Emergency Propulsion of a Vessel in the Event of Loss of the Full Serviceability of the Diesel Main Engine. Energies, 15(8), 2833. https://doi.org/10.3390/en15082833.

[31] McKenna, M.F., Ross, D., Wiggins, S.M., Hildebrand, J.A. (2012). Underwater radiated noise from modern commercial ships. The Journal of the Acoustical Society of America, 131, 92-103. https://doi.org/10.1121/1.3664100.

[32] Mironiuk W. (2015). Model tests of the dynamic ship heeling in terms of maritime transport safety. Archives of Transport, 33(1), 69-80. https://doi.org/10.5604/08669546.1160928.

[33] Mou, J.M., et al. (2019). Vessel traffic safety in busy waterways: A case study of accidents in western shenzhen port. Accident Analysis & Prevention, 123, 461-468, https://doi.org/10.1016/j.aap.2016.07.037.

[34] O'Kelly-Lynch, P.D., et al. (2020). Offshore conversion of wind power to gaseous fuels: Feasibility study in a depleted gas field. Proceedings of the Institution of Mechanical Engineers, Part A. Journal of Power and Energy, 234 (2), 226-236, https://doi.org/10.1177/0957650919851001.

[35] Önden, İ., Deveci, M., Çancı, M., Çal, M., & Önden, A. (2023). A spatial analytics decision support system for analyzing the role of sea transport in public transportation. Decision Analytics Journal, 6, 100149. https://doi.org/10.1016/j.dajour.2022.100149.

[36] Pelot, R., Plummer, L. (2008). Spatial analysis of traffic and risks in the coastal zone. Journal of Coastal Conservation, 11 (201). https://doi.org/10.1007/s11852-008-0026-7.

[37] Pleskachevsky, A., Tings, B., Wiehle, S., Imber, J., & Jacobsen, S. (2022). Multiparametric sea state fields from synthetic aperture radar for maritime situational awareness. Remote Sensing of Environment, 280, 113200. https://doi.org/10.1016/j.rse.2022.113200.

[38] Qu, J., Liu, R. W., Guo, Y., Lu, Y., Su, J., & Li, P. (2023). Improving maritime traffic surveillance in inland waterways using the robust fusion of AIS and visual data. Ocean Engineering, 275, 114198. https://doi.org/10.1016/j.oceaneng.2023.114198.

[39] Queiroz Pereira, W., Correia Dantas, W. (2019). From seabathing to sports onbeaches and sea areas. Sociedade & Natureza, 31, 1-21, https://doi.org/10.14393/SN-31-2019-46981.

[40] Ruiz-Salmón, I., et al. (2021). Life cycle assessment of fish and seafood processed products – A review of methodologies and new challenges. Science of the Total Environment, 761, 144094. https://doi.org/10.1016/j.scitotenv.2020.144094.

[41] Smirnova, O.V. (2018). Situation Awareness for Navigation Safety Control. TransNav: International Journal on Marine Navigation and Safety of Sea Transportation, 12 (2), 383-388, https://doi.org/10.12716/1001.12.02.20.

[42] Stach, T., Kinkel, Y., Constapel, M., & Burmeister, H. C. (2023). Maritime Anomaly Detection for Vessel Traffic Services: A Survey. Journal of Marine Science and Engineering, 11(6), 1174. https://doi.org/10.3390/jmse11061174.

[43] Tarnawski, J., Buszman, K., Woloszyn, M., Rutkowski, T. A., Cichocki, A., & Józwiak, R. (2021). Measurement campaign and mathematical model construction for the ship Zodiak magnetic signature reproduction. Measurement, 186, 110059. https://doi.org/10.1016/j.measurement.2021.110059.

[44] Tesei, A., et al. (2015). Passive acoustic surveillance of surface vessels using tridimensional array on an underwater glider. In OCEANS 2015-Genova (pp. 1-8). IEEE. https://doi.org/10.1109/OCEANS-Genova.2015.7271573.

[45] Ustalli, N., Villano, M. (2022). High-Resolution Wide-Swath Ambiguous Synthetic Aperture Radar Modes for Ship Monitoring. Remote Sensing, 14, 3102. https://doi.org/10.3390/rs14133102.

[46] Van Elden, S., Meeuwig, J. J., Hobbs, R. J., & Hemmi, J. M. (2019). Offshore oil and gas platforms as novel ecosystems: A global perspective. Frontiers in Marine Science, 6, 548. https://doi.org/10.3389/fmars.2019.00548.

[47] Voytyuk, O. (2022). The Baltic Pipe and its impact on energy security in Central and Eastern Europe. Polityka Energetyczna-Energy Policy Journal, 89-108. https://doi.org/10.33223/epj/145554.

[48] Watson, J. T., & Haynie, A. C. (2016). Using vessel monitoring system data to identify and characterize trips made by fishing vessels in the United States North Pacific. PloS one, 11(10), e0165173. https://doi.org/10.1371/journal.pone.0165173.

[49] Widyaningrum, D., & Masruroh, N. A. (2012). Development of the sea fishery supply chain performance measurement system: a case study. International Journal of Supply Chain Management, 1(3), 20-32. https://doi.org/10.59160/IJSCM.V1I3.644.

[50] Wołoszyn, M., Buszman, K., Rutkowski, T., Tarnawski, J., & Rodrigo Saura, F. J. (2022). An analytical four-layer horizontal electric current dipole model for analysing underwater electric potential in shallow seawater. Scientific Reports, 12(1), 8727. https://doi.org/10.1038/s41598-022-12645-z.

[51] Wu, X., Roy, U., Hamidi, M., Craig, B.N. (2020). Estimate travel time of ships in narrow channel based on AIS data. Ocean Engineering, 202, 106790. https://doi.org/10.1016/j.oceaneng.2019.106790.

[52] Xin, X., Liu, K., Loughney, S., Wang, J., Li, H., Ekere, N., & Yang, Z. (2023). Multi-scale collision risk estimation for maritime traffic in complex port waters. Reliability Engineering & System Safety, 240, 109554. https://doi.org/10.1016/j.ress.2023.109554.

[53] Zhang, G., et al. (2019). Giant discoveries of oil and gas fields in global deepwaters in the past 40 years and the prospect of exploration. Journal of Natural Gas Geoscience, 4 (1), 1-28, https://doi.org/10.1016/j.jnggs.2019.03.002.

[54] Zhang, T., Zeng, T., & Zhang, X. (2023). Synthetic aperture radar (SAR) meets deep learning. Remote Sensing, 15(2), 303. https://doi.org/10.3390/rs15020303.